Available online at www.sciencedirect.com
ScienceDirect
Ceramics International 35 (2009) 571–577
CERAMICS INTERNATIONAL
www.elsevier.com/locate/ceramint

Iron role on mechanical properties of ceramics with clays from Ivory Coast

J.Y.Y. Andji [a], A. Abba Toure [a], G. Kra [a], J.C. Jumas [b], J. Yvon [c], P. Blanchart [d,*]

[a] *Mineral Chemistry Laboratory (Ufr-ssmt/Cocody University), 22 BP 582 Abidjan 22, Ivory Coast*
[b] *LAMMI, Montpellier II University, France*
[c] *LEM, ENSG/INPL, Vandoeuvre Lès Nancy, France*
[d] *GEMH-ENSCI, Limoges, France*

Received 20 August 2007; received in revised form 3 December 2007; accepted 10 January 2008
Available online 8 April 2008

Abstract

Three clays from Gounioubé deposits were used for the manufacture of floor tiles. The strength distributions by the Weibull statistical model are interpreted in relation to clay chemical and mineralogical compositions and particularly to the iron role by Mössbauer spectroscopy. With clays without additions, results of mechanical strength of sintered materials show that clays alone are not really suitable for the manufacture of ceramics. But clay calcite mixes (10 wt% of $CaCO_3$) favor a significant increase of mechanical resistance, which are similar to used standards. This behavior is due to the formation of a three-dimensional network of anorthite crystals within the silico-aluminate materials. Beside the anorthite role, the iron oxide content of the clays influences the mechanical strength. With Gounioubé clays, it is shown that the increase of iron content in clays causes a decrease of the ceramic strength. This behavior is related to the clay compositions, which contain iron in the form of goethite. During the thermal transformations, part of the iron is involved in both the structural transformations and the densification phenomenon of the silico-aluminate phase. But the most part of iron readily transforms into hematite crystallites, which are embedded within the silico-aluminate. They accentuate the heterogeneous nature of the material and favor the decrease of the mechanical strength.

Keywords: A. Sintering; C. Strength; C. Toughness; D. Clays

1. Introduction

At present, many ceramics are manufactured from mixtures of mineral raw materials, which are shaped by compaction and sintered at high temperature. In general, silico-aluminate raw materials are complex natural mixtures of minerals which properties are appropriated for the manufacture of common ceramics (bricks, roof tiles, dinner wares, sanitary wares, floor tiles and glasses). To select the appropriate raw materials, users are always looking for specific criteria, which are related either to the behavior during the various stages of manufacturing and to the overall chemical composition.

In Ivory Coast, ceramics for building use 70% of imported products, mainly floor tiles and sanitary wares. Taking into account the availability of kaolinitic clay deposits in the Gounioubé area, it is interesting to investigate the potential use of these clays for the production of ceramic wares, particularly ceramics for building.

The aim of this study is to explore the possible manufacturing of ceramic floor tiles, composed of three clays selected in Gounioubé deposits, which are located at about 15 km of Abidjan, in the Anyama prefecture. The study will investigate two main points:

- the physicochemical and thermal transformations of clays, which are useful information in the manufacturing of ceramics;
- the influence of the chemical composition and mainly the iron content on the mechanical properties of the fired products.

2. Materials and methods

The three clays are referenced G5, G9 and G13. They are very representative of kaolinitic clays available in Gounioubé

* Corresponding author at: ENSCI, Limoges, 47-73 Avenue Albert Thomas, 87065 Limoges, France. Tel.: +33 5 55 45 22 11; fax: +33 5 55 79 09 98.
E-mail address: philippe.blanchart@unilim.fr (P. Blanchart).

0272-8842/$34.00
doi:10.1016/j.ceramint.2008.01.007

Table 1
Chemical composition of the raw materials G5, G9 and G13

Sample	G5	G9	G13
SiO_2	48.58	46.45	40.62
Al_2O_3	26.28	31.47	25.38
Fe_2O_3	4.78	2.61	15.66
TiO_2	3.35	2.93	2.49
K_2O	0.84	0.59	0.29
P_2O_5	0.96	0.52	0.35
MgO	0.06	0	0
CaO	0.15	0.11	0
Na_2O	0	0.12	0
P.F.	14.64	15.01	15.04
Total	99.64	99.81	99.83

deposits in Ivory Coast [1]. The raw clays from quarries were preliminary dried at 100 °C and all experiments were performed with the size fraction below 100 μm. Tables 1 and 2 give the chemical compositions (by ICP) and mineralogical compositions of clays (by XRD and calculation from the chemical composition). The major minerals are kaolinite, quartz and mica. Iron minerals are under the form of goethite in the three clays. The occurrence of gibbsite in clay from Ivory Coast is due to soil leaching during a hot tropical climate [2].

Floor tiles samples were manufactured at the laboratory scale, using either the raw materials without additions and the same raw materials with the addition of 10 wt% of calcite. Homogenized raw materials with 5 wt% of water were agglomerated to form granules before die pressing and sintering at 1100 °C with a heating rate of 5 °C min^{-1}.

Dilatometric analysis was used to characterize the sintering behavior of materials. Structural transformations during sintering were followed by X-ray diffraction, using a Bruker diffractometer (D8) with a cobalt source ($\lambda = 1.7789$ Å). Measurements of mechanical resistance were carried out by the three points method, with a Schenk RMC machine.

Because ceramic materials present variations in their microstructures, it is necessary to consider a distribution of strengths. The calculation of the related failure probability considers the widely used model, which is the Weibull's two-parameter equation [3]. It relates the cumulative probability of survival P_s to the stress σ in a sample volume V, and to the Weibull shape factor m and the normalizing factor σ_0.

$$P_s = \frac{N+1-i}{N+1} = \exp\left\{-\left(\frac{\sigma_i}{\sigma_0}\right)^m\right\} \quad (1)$$

In general, it is widely accepted that the m parameter is related to the material reliability.

For measurements of fracture toughness, the method of single edge notched beam (SENB) was used. The K_{Ic} parameter was calculated from the experimental fracture stress σ_t and the Y and a_0 parameters, which depend on both the test method and the specimen geometry:

$$K_{Ic} = \frac{\sigma_t Y}{a_0} \quad (2)$$

The influence of iron on the mechanical resistance was studied by ^{57}Fe Mössbauer spectroscopy. Spectra were collected at room temperature with a EG&G spectrometer with a ^{57}Co(Rh) source. The velocity scale is calibrated with reference to the magnetic sextet spectrum of a metallic iron foil absorber and isomer shifts are given with respect to the centre of this spectrum. All spectra were refined using the ISO program [4] and the convergence of fits was calculated with the χ^2 test.

3. Results and discussion

3.1. Tests carried out with raw material without addition

Dilatometric analyses are in Fig. 1. Curves of G5, G9 and G13 are similar to curves of pure kaolinite [5]. The main variations in curves are the followings:

- Dilation of G5, G9 and G13 at temperature upto about 450 °C.
- A first densification between 500 °C and 600 °C, simultaneously to the dehydroxylation of kaolinite. This phenomenon is very accentuated for G9 and less accentuated for G5 and G13. The extent of densification during dehydroxylation is related to the high kaolinite content in G9 (77.5 wt%), and to its lower content in G5 (51.74 wt%) and in G13 (51.04 wt%).
- The α to β transformation of quartz at 573 °C, is very accentuated with G5 and G13 because they contain more quartz than G9.
- The first densification between 600 and 950 °C results from the progressive structural reorganization of metakaolinite after dehydroxylation. Densification is more accentuated with G9 (highest kaolinite content) than with G5 and G13. Besides, the extent of densification depends on the presence of mica, which dehydroxylates progressively to form a high temperature phase above 600 °C. In general, the cell volume of mica increases with temperature, which partially compensates densification from kaolinite recrystallization.
- A second densification between 950 and 1000 °C, which is obviously more accentuated with G9, because it contains more kaolinite.

Table 2
Calculated mineral compositions from data of chemical analyses

Sample	Kaolinite	Quartz	Anatase	Mica	Smectite	Goethite	Gibbsite	P.F.	Total
G5	51.74	12.46	2.78	6.03	11.2	3.19	9.73	2.42	99.55
G9	77.5	2.1	2.18	3.81	6	1.32	3.39	3.36	99.66
G13	51.04	6.4	2.27	4.38	11.49	15.19	4.56	2.45	97.78

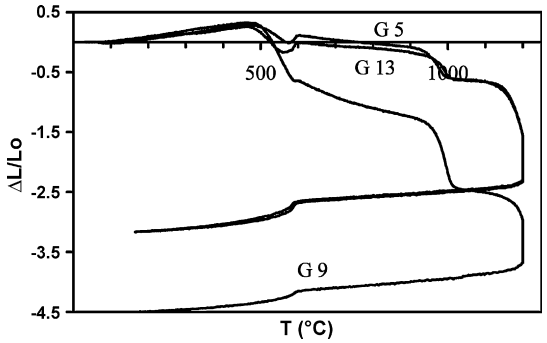

Fig. 1. Dilatometric curve of G9, G5 and G13 clays.

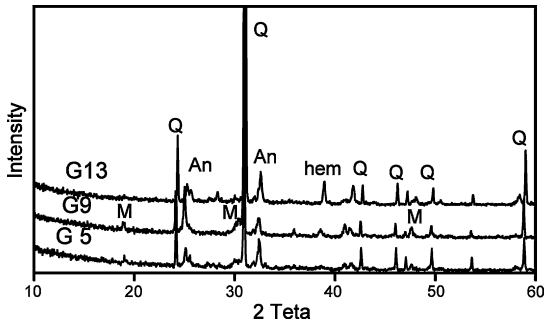

Fig. 2. X-ray patterns of G5, G9 and G13 with 10% of $CaCO_3$ and fired at 1100 °C, 1 h. Q: quartz; An: anorthite; hem: hematite; M: mullite.

- A small densification between 1050 and 1150 °C, the extent of which is limited by the simultaneous densifications from sintering and crystalline growth [6]. The high densification rate is mainly related to variations in mineralogical compositions and to phase morphologies in the initial mixture of raw materials. For G9, densification is less accentuated because of the higher content of kaolinite and the lower content of mica and smectite minerals. Curves of G5 and G13 are similar, which is in relation to comparable contents of argillaceous minerals in the two clays. Beside the clay mineral role, it can be supposed the effect of iron minerals. A first observation of G9 and G13 curves evidences their similar variations, whereas the Fe_2O_3 contents are very different. It could be related to Fe_2O_3 under the form of hematite, in which interaction with surrounding minerals is limited. This point will be discussed later and supported by X-ray diffraction studies after heat treatments up to 1300 °C.
- During cooling, the volume variation at about 573 °C is from the β to α transformation of the remaining quartz, whose larger grains has a low reactivity with surrounding phases.

The mechanical characterizations of ceramic tiles with the three raw materials after shaping and sintering at 1100 °C were characterized by three-point bending tests up to the rupture. Average values of fracture stress of G5, G9 and G13 samples are very low (0.4–1.2 MPa) and are much lower than what required for manufactured tiles. Standards indicate that stress values at material fracture must be more than 21 MPa for clay products and more than 55 MPa for vitrified ceramic wares. These results point out the limited importance of the materials in building. Consequently, raw materials from Gounioubé quarries were mixed with calcite to manufacture ceramics tiles.

3.2. Clay materials mixed with 10 wt% of $CaCO_3$

Structural transformations with temperature of clay–calcite mixes were studied by X-ray diffraction. X-ray patterns of G5, G9 and G13 mixes are given in Fig. 2. Crystallized phases are similar for the three samples and the presence of anorthite, mullite, hematite and quartz phases is evidenced.

Anorthite is the end member of a two stages reaction sequence, which gives the most stable phase at the sintering temperature, according to Sigg [7], Sandoval and Ibanez [8]:

First, free silica reacts with calcite:

$$CaCO_3 + SiO_2 \rightarrow CaSiO_3 + CO_2 \quad (960-980\,^{\circ}C)$$

Then anorthite crystallize from wollastonite and alumina from clay minerals, according to the following reaction:

$$CaSiO_3 + Al_2O_3 + SiO_2 \rightarrow CaAl_2Si_2O_8$$

On diffraction patterns, wollastonite is not detected because it is a transient phase only detected at contact points of quartz and calcite [9] in heterogeneous microstructures.

Simultaneously to the reaction sequence, hematite phase in clearly evidenced in G13 and G9 materials.

Three-points bending tests of a set of 50 samples were achieved to ensure the validity of the statistical treatment of data. Results of survival probabilities against the maximum stresses are represented in Fig. 3. The large distribution of the maximal constraints is obvious and the maximum rupture stress is in the range 10–20 Mpa. These stress values are 10 times higher than those obtained with sintered clays without additions and are similar to that required by standards of manufactured floor tiles from clay products. Moreover, it should be noted that the mechanical resistance decreases when the quantity of iron increases. Correspondingly, tiles carried out with the G9 clay containing the lowest iron quantity are the most resistant materials. It must be noted that these significant strength values are obtained notwithstanding the high porosity, which range from 36.2 to 41.8%.

Beside iron role, the strength variation of the fired material is also related to the material microstructure and mainly the pore fraction, as evidenced by Kingery et al. [10] and very recently

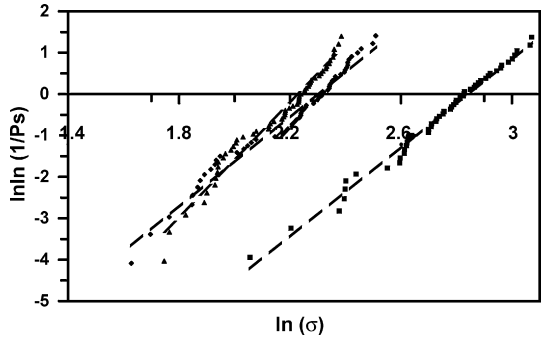

Fig. 3. Probability of survival against bending stress up to fracture, of the G5 (rhombs), G9 (square) and G13 (triangle) materials.

Table 3
Weibull modulus and interval of fracture stress for the three sintered clays with 10 wt% of calcite in relation to the iron oxide content in clay

	G9 (1.67%)	G5 (3.44%)	G13 (18.27%)
m	5.4	5.5	6.9
Stress interval (MPa)	7.8–21.5	5.1–12.3	5.1–10.8

with refractory ceramics [11]. In all cases, the empirical relationships which is generally used relates the strength σ to the porosity p:

$$\sigma = \sigma_o \exp(-n\,p) \quad (3)$$

Although it is an exponential law, the curve slope is very weak at high porosity, above 20 vol%. Given the small difference between porosities of our samples, it can be assumed that the strength variation is highly correlated to the crystalline phases quantities and their spatial repartition.

The distributions of the probabilities of survival are given in Fig. 3. They are calculated from the experimental rupture stresses, with the assumption of a uni-modal distribution of stresses. The satisfactory fit of data points out the existence of a single population of defects within microstructures. Close values of m Weibull modulus (Table 3) are obtained with the three samples. The relatively high values of m point out the limited interval of possible fracture stresses. We also note that the m Weibull modulus does not vary much with the iron quantity.

Fracture toughness of materials is given in Table 4. The relatively low values must be compared to data published for common ceramic as porcelain and glasses [12]. The fracture toughness increases with the iron oxide concentration, up to 3.44 wt.% (G5 and G9 materials) and decreases at higher iron oxide content (G13; 18.27 wt%). This change against the quantity of iron oxide seems to be correlated with the structural and microstructural transformations during sintering where iron compounds are involved.

3.3. Characterization by Mössbauer spectroscopy

Mössbauer spectroscopy was used to observe the iron role during thermal transformations. For spectrum interpretation, we used one or two broad doublets (Fig. 4), characterized by an isomer shift (ISD) and a quadrupole splitting (QSD).

In kaolinite mineral, Al can be partially substituted by structural Fe. From Mössbauer investigations, the presence of octahedrally co-ordinated Fe^{III} is well established [13] and Fe^{II} can be substituted trioctahedrally in the structure [14,15].

Table 4
Values of fracture toughness for the samples G5 G9 and G13 in relation to iron oxide content in clays

	K_{Ic} (MPa m$^{-1/2}$)
G5 + 10% $CaCO_3$ (1.67%)	0.47
G9 + 10% $CaCO_3$ (3.44%)	0.81
G13 + 10% $CaCO_3$ (18.27%)	0.42

Experimental parameters of Mössbauer spectra corresponding to Fe^{III} in kaolinite tetrahedral sites are published in [16].

Beside structural Fe, iron oxides or hydroxides are often detected with kaolinitic clays [17]. The most widely occurring Fe oxide is hematite, mostly as very fine particles [18] or goethite adsorbed on kaolinite surfaces [14].

The Mössbauer spectrums of G5, G9 and G13 samples were obtained with clays after various treatments: (a) bleaching by CDB (sodium citrate–dithionite–bicarbonate) to remove extractable Fe; (b) mixing with 10 wt% of calcite; (c) heating at 1100 and 1300 °C (Fig. 4). Spectra characteristics are reported in Table 5. Spectra of the G5, G9, and G13 samples before and after bleaching were simulated with a central doublet with low values of ISD (0.36 mm s^{-1}) and a QSD value of 0.5 mm s^{-1}. Data point out to the existence of Fe^{3+} ions, as it is generally observed in the kaolinite structure, whose typical data are ISD ~0.35 mm s^{-1} and QSD ~0.50–0.65 mm s^{-1} [13,14,19]. Beside the main doublet, a smaller doublet has higher values of ISD (1.04–1.06 mm s^{-1}) and a QSD value in the range 2.0–2.51 mm s^{-1}. It corresponds to ferrous ions Fe^{2+} in the kaolinite structure.

The contribution of different iron type is calculated from relative surfaces of respective sub spectra, which are related to atom quantities. They are reported in Table 5 where the predominance of Fe^{3+} in tetrahedral and/or octahedral sites is evidenced.

After firing at the 1300 °C temperature, Mössbauer spectra of G5, G9 and G13 show significant differences:

- G5 spectrum has a single doublet related to Fe^{3+}. All iron atoms from kaolinite and from other iron compounds are Fe^{3+}.
- G9 spectrum has a main doublet related to Fe^{3+}. It accounts for 87.4 wt% of the whole iron content. A sextuplet is related to magnetic iron of hematite in quantity of 12.6 wt%.
- G13 spectrum can be simulated with a doublet of Fe^{3+} and a sextuplet related to magnetic iron of hematite, in quantity of 34.8 and 65 wt%, respectively.

All spectra of clays mixed with 10% of $CaCO_3$ and sintered at 1100 °C reveal the presence of hematite in significant quantity. The quantities are higher than that of clay fired at 1300 °C temperature for the three samples.

The position of Fe^{2+} ions in kaolinite structures can be discussed against QSD values of doublets in G5 and G13 spectra (Table 6). Since QSD values are 2.2 and 2.0 mm s^{-1}, respectively, they are lower than those published by Murad and Wagner with different clays (2.5–2.8 mm s^{-1}) [19] and with very pure kaolinite (2.53 mm s^{-1}; ISD = 1.1 mm s^{-1}). Consequently, both clays are not supposed to contain Fe^{2+}. For G9, QSD (2.5 mm s^{-1}) is close to Murad and Wagner data and ferrous ions are supposed to be substituted in the kaolinite structure.

The heat treatment at 1100 and 1300 °C, favors the change of Fe^{2+} ions to Fe^{3+} either in the silico-aluminate phase or in hematite. At 1100 °C, clays with calcite contain the most part of Fe^{3+} as hematite (Table 5). The ratio of Fe^{3+} in structural

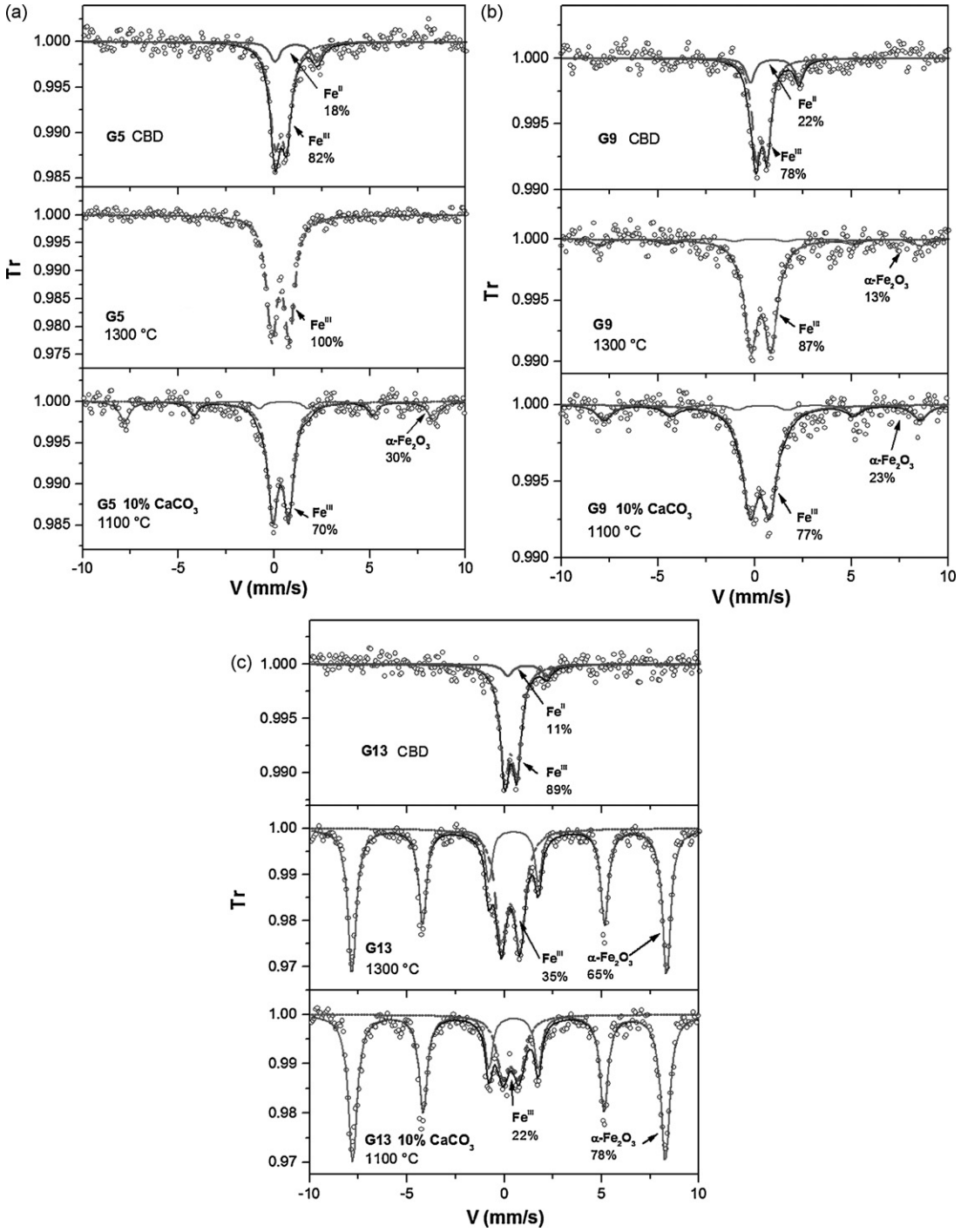

Fig. 4. Mössbauer spectra of samples G5 (a), G9 (b) and G13 (c), after treatment with CBD, fired at 1300 °C and mixed with 10% of $CaCO_3$ and fired at 1100 °C.

position to hematite decreases with the increase of iron oxide content in initial clays. This ratio attains 77% in G9 and 70% in G5, but decreases to 22% in G13. In Gounioubé clays, it can be supposed a possible nucleation and growth phenomenon of hematite in the presence of other phases as Ca, Al silicates.

At 1300 °C, the clays alone present different behaviors. With G5, the totality of iron is transformed into structural Fe^{3+}. This global transformation was already reported by Castelein et al. [20], which describes the drastic reduction of hematite and other iron phases above 1000 °C, to form structural Fe^{3+} by the interaction with surrounding phases from kaolinite. In general, the rate of inter-reaction increases when a high heating rate is used.

In G9 and G13 at 1300 °C, Fe^{3+} coexist with hematite. But the hematite to Fe^{3+} ratio is higher in G13 than in G9, which could be explained by the presence of more iron minerals in G13 than in G9. In G13, the iron oxide (18.27 wt%) is mainly from goethite, which readily oxidizes into hematite at high temperature. In G9, the very few goethite content (1.27 wt%) limits the quantity of hematite, which is crystallized at 1300 °C.

Table 5
Characteristics of Mössbauer spectra in relation to sample treatments

Ech.	ISD (mm/s)	QSD (mm/s)	Line Width (mm/s)	Contribution (%)	H (T)	Attribution
G5-CDB	0.36 (2)	0.60 (5)	0.64 (4)	82	–	Fe^{III}
	1.16 (5)	2.2 (1)	0.64 (4)	18		Fe^{II}
G5-1300 °C	0.34 (1)	0.91 (1)	0.64 (1)	100	–	Fe^{III}
G5-10 wt% $CaCO_3$; 1100 °C	0.34 (1)	0.82 (2)	0.64 (3)	69.8	–	Fe^{III}
	0.36 (5)	−0.15 (3)	0.64 (3)	30.2	49.9 (2)	α-Fe_2O_3
G9-CDB	0.37 (2)	0.56 (2)	0.52 (8)	78.5	–	Fe^{III}
	1.04 (5)	2.51 (8)	0.52 (8)	21.5	–	Fe^{II}
G9-1300 °C	0.33 (2)	1.04 (4)	0.81 (4)	87.4	–	Fe^{III}
	0.28 (13)	–	0.89 (7)	12.6	51.7 (1)	α-Fe_2O_3
G9-10 wt% $CaCO_3$; 1100 °C	0.28 (2)	1.01 (2)	0.95 (8)	77.3	–	Fe^{III}
	0.39 (11)	–	0.95 (8)	22.7	50.8 (5)	α-Fe_2O_3
G13-CDB	0.33 (1)	0.63 (2)	0.57 (4)	89.3	–	Fe^{III}
	1.2 (1)	2.0 (2)	0.57 (4)	10.7	–	Fe^{II}
G13-1300 °C	0.32 (1)	0.95 (1)	0.68 (2)	34.8	–	Fe^{III}
	0.37 (2)	−0.11 (2)	0.51 (2)	65.2	50.2 (1)	α-Fe_2O_3
G13-10 wt% $CaCO_3$; 1100 °C	0.35 (3)	0.82 (4)	0.76 (6)	21.8	–	Fe^{III}
	0.36 (2)	−0.12 (2)	0.55 (2)	78.2	49.9 (1)	α-Fe_2O_3

Table 6
Parameters deduced from the Mössbauer spectra acquired at 25 °C in comparison to data from Murad and Wagner (1993)

	Fe^{3+}		Fe^{2+}	
	ISD (mm s^{-1})	QSD (mm s^{-1})	ISD (mm s^{-1})	QSD (mm s^{-1})
Murad and Wagner (1993)	0.30–0.36	0.50–0.66	1.1–1.2	2.5–2.8
G5 (CBD)	0.36	0.60	1.16	2.2
G9 (CBD)	0.37	0.56	1.04	2.51
G13 (CBD)	0.33	0.63	1.2	2.0

The iron role on the mechanical properties of clay with calcite fired products is shown with strength and fracture toughness data in Fig. 3 and Table 4. In general, strength values decrease with the increase of the iron content, but fracture toughness varies in a more complex way.

Accordingly to Mössbauer results with clay–calcite mixes fired at 1100 °C, we observe the increase of hematite in clays G9 (22.7%), G5 (30.2%) and G13 (78.2%). Simultaneously, Fe^{3+} decrease from G9 (77.3%); G5 (69.8%) to G13 (21.8%).

During sintering between 800 and 900 °C, calcite is decomposed into CaO and CO_2. CaO reacts with the metakaolinite amorphous phase, which quantity decreases with temperature. Gehlenite and anorthite phases are subsequently crystallized while the formation of wollastonite is not observed. According to Traoré et al. [21], Fe^{3+} favors the transformation of metakaolinite into gehlenite and anorthite. The mechanical resistance of ceramics is increased by the strengthening effect of phase interconnection in microstructures [22]. Besides, the densification of materials is enhanced, simultaneously to the progressive formation of aluminium silicates (gehlenite, anorthite) [23,24]. With our clay materials with calcite, since G9 contains the highest structural Fe^{3+} content, after sintering at 1100 °C (77%), it is readily correlated with a high mechanical resistance. Correspondingly, G5 (69.8%) and G13 (21.8%) present lower strength values.

4. Conclusion

The use of clays from Gounioubé deposits as ceramic components were carried out with clays and clays mixed with 10% of calcite, followed by sintering at 1100 and 1300 °C.

The mechanical resistances of sintered bars from G5, G9 and G13 clays point out weak maximum strength, in the range of 0.4–1.2 MPa. All samples cannot be used for the manufacture of floor tiles. In a different way, clay mixed with 10% of calcite favors the increase of mechanical resistances up to 10–20 Mpa that is close to sintered clay products for building. The fracture toughness of clay–calcite mixes ranges from 0.42 to 0.81 MPa $m^{-1/2}$. They are slightly lower to that of common ceramics but they are representative of heterogeneous ceramics.

The influence of iron on material properties point to the detrimental role of hematite on the mechanical resistances. It is related to the goethite role in Gounioubé clay, which readily transforms to hematite during the thermal treatment. Since Fe^{3+} quantity in silico-aluminate phase is low, it does not act effectively in sintering. Besides, hematite crystallites are embedded in the silico-aluminate phase, which favors the heterogeneous character of the material and decreases the mechanical strength.

References

[1] J.Y.Y. Andji, J. Sei, A. Abba Toure, G. Kra, D. Njopwouo, Caractérisation Minéralogique de quelques échantillons d'argile du site de Gounioube (Cote D'ivoire), J. Soc. Ouest-Afr. Chim. 011 (2001) 143–166.

[2] L. Herrmanna, N. Anongrakb, M. Zareia, U. Schulera, K. Spohrera, Factors and processes of gibbsite formation in Northern Thailand, Catena 71 (2) (2007) 279–291.

[3] W. Weibull, A statistical distribution function of wide applicability, J. Appl. Mech. 18 (3) (1951) 253.

[4] W. Kündig, Nucl. Instrum. Methods Phys. Res. 75 (1969) 336–340.

[5] D. Bernache-Assollant, Chimie physique du frittage, Ed. Hermès, Paris, 1993.

[6] J. Rocha, J. Klinowski, ^{29}Si and ^{27}Al magic-angle-spinning MNR studies of the thermal transformation of kaolinite, J. Chem. Soc. Commun. (1991) 582–584.

[7] J. Sigg, Les produits de terre cuite, Ed. Septima, Paris, 1995.

[8] F. Sandoval, A. Ibanez, Fast-firing wollastonite based wall tiles bodies, Am. Ceram. Soc. Bull. 78 (3) (1999) 72–75.

[9] D. Piponier, F. Bechtel, D. Florin, J. Molera, M. Schvoerer, M. Vendrell, Apport de la cathodoluminescence à l'étude des transformations de phases cristallines dans des céramiques kaolinitiques carbonates, Key Eng. Mater. 132–136 (1986) 1470–1473.

[10] W.D. Kingery, H.K. Bowen, D.R. Uhlmann, Introduction to Ceramics, 2nd ed., John Wiley and Sons/Wiley-Interscience, New York, 1976.

[11] A. Atkinson, P. Bastid, Q. Lui, Mechanical properties of magnesia–spinel composites, J. Am. Soc. 90 (8) (2007) 2489–2496.

[12] H. Zanzoun, Optimisation des étapes d'élaboration de céramiques à partir d'argiles du Maroc, Thèse de Doctorat 3ème cycle de l'Université Ain Chock, Casablanca, 1995.

[13] P.J. Malden, R.E. Meads, Substitution by iron in kaolinite, Nature 215 (1967) 844–846.

[14] D.A. Jefferson, M.J. Tricker, A.P. Winterbottom, Electron microscopy and Mössbauer spectroscopic studies of iron stained kaolinite minerals, Clay Clay Miner. 23 (1975) 355–360.

[15] A.H. Cuttler, The behavior of a synthetic ^{57}Fe doped kaolin: Mössbauer and electron paramagnetic resonance studies, Clay Miner. 15 (1980) 429–444.

[16] S. Petit, A. Decarreau, Hydrothermal synthesis and crystal chemistry of iron-rich kaolinites, Clay Miner. 25 (1990) 181–196.

[17] C.S. Hogg, P.J. Malden, R.E. Meads, Identification of iron containing impurities in naturral kaolinites using the Mössbauer spectroscopy effect, Miner. Mag. 40 (1975) 89–96.

[18] C. Janot, H. Gibert, C. Tobias, Caracterisation de kaolinites ferrifères par spectroscopie Mösbauer, Bull. Soc. Fr. Miner. Crystallogr. 96 (1973) 281–291.

[19] E. Murad, U. Wagner, Mössbauer spectra of kaolinite, halloysite and the firing products of kaolinite: new results and a reappraisal of published work, Neues Jahrbuch Miner. Abh. 162 (1991) 281–309.

[20] O. Castelein, B. Soulestin, J.P. Bonnet, P. Blanchart, The influence of heating rate on the thermal behavior and mullite formation from a kaolin raw material, Ceram. Int. 27 (5) (2001) 517–522.

[21] K. Traoré, T.S. Kabré, P. Blanchart, Géhlénite and anorthite crystallisation from kaolinite and calcite mix, Ceram. Int. 26 (2003) 715–720.

[22] V.M. Sglavo, S. Maurina, A. Conci, A. Saviati, G. Carturan, G. Cocco, Bauxite 'red mud' in the ceramic industry. Part 2. Production of clay-based ceramics, J. Eur. Ceram. Soc. 20 (3) (2000) 245–252.

[23] O. Castelein, J.C. Jumas, J. Fourcade, J.P. Bonnet, P. Blanchart, Iron distribution in a kaolin raw material, by Mössbauer spectroscopy, influence of temperature and temperature rate, J. Eur. Ceram. Soc. 22 (11) (2002) 1767–1773.

[24] S.J.G. Sousa, J.N.F. Holanda, Development of red wall tiles by the dry process using Brazilian raw materials, Ceram. Int. 31 (2) (2005) 215–222.